J Arid Land (2025) 17(1): 58–73
doi: 10.1007/s40333-025-0002-1; CSTR: 32276.14.JAL.02500021

Science Press Springer-Verlag

Spatiotemporal variation and influencing factors of desertification sensitivity on the Qinghai-Xizang Plateau, China

PAN Meihui[1,2*], CHEN Qing[1], LI Chenlu[1], LI Na[1], GONG Yifu[1]

[1] College of Geography and Environmental Science, Northwest Normal University, Lanzhou 730070, China;
[2] Key Laboratory of Resource Environment and Sustainable Development of Oasis, Northwest Normal University, Lanzhou 730070, China

Abstract: Due to irrational human activities and extreme climate, the Qinghai-Xizang Plateau, China, faces a serious threat of desertification. Desertification has a detrimental effect on the ecological environment and socioeconomic development. In this study, the desertification sensitivity index (DSI) model was established by integrating the spatial distance model and environmentally sensitive area index evaluation method, and then the model was used to quantitatively analyze the spatial and temporal characteristics of desertification sensitivity of the Qinghai-Xizang Plateau from 1990 to 2020. The results revealed that: (1) a general increasing tendency from southeast to northwest was identified in the spatial distribution of desertification sensitivity. The low-sensitivity areas were mostly concentrated in the Hengduan and Nyaingqêntanglha mountains and surrounding forest and meadow areas. The high-sensitivity areas were located mainly in the Kunlun and Altun mountains and surrounding decertified areas. The center of gravity of all types of desertification-sensitive areas moved to the northwest, and the desertification sensitivity showed a decreasing trend as a whole; (2) the area of highly sensitive desertification areas decreased by 8.37%, with extreme sensitivity being the largest change among the sensitivity types. The desertification sensitivity transfer was characterized by a greater shift to lower sensitivity levels (24.56%) than to higher levels (2.03%), which demonstrated a declining trend; (3) since 1990, the change in desertification sensitivity has been dominated by the stabilizing type I (29.30%), with the area of continuously increasing desertification sensitivity accounting for only 1.10%, indicating that the management of desertification has achieved positive results in recent years; and (4) natural factors have had a more significant impact on desertification sensitivity on the Xizang Plateau, whereas socioeconomic factors affected only localized areas. The main factors influencing desertification sensitivity were vegetation drought tolerance and aridity index. Studying spatiotemporal variations in desertification sensitivity and its influencing factors can provide a scientific foundation for developing strategies to control desertification on the Qinghai-Xizang Plateau. Dividing different desertification-sensitive areas on the basis of these patterns of change can facilitate the formulation of more targeted management and protection measures, contributing to ecological construction and sustainable economic development in the area.

Keywords: desertification sensitivity; geodetector; gravity center transfer model; spatiotemporal change; Qinghai-Xizang Plateau

Citation: PAN Meihui, CHEN Qing, LI Chenlu, LI Na, GONG Yifu. 2025. Spatiotemporal variation and influencing factors of desertification sensitivity on the Qinghai-Xizang Plateau, China. Journal of Arid Land, 17(1): 58–73. https://doi.org/10.1007/s40333-025-0002-1; https://cstr.cn/32276.14.JAL.02500021

*Corresponding author: PAN Meihui (E-mail: panmh@nwnu.edu.cn)
Received 2024-05-14; revised 2024-10-22; accepted 2024-10-28

1 Introduction

Desertification is a process, in which land becomes degraded due to unfavorable natural conditions or excessive human activities in arid and semi-arid areas (UNCCD, 1994). China has become one of the countries most affected by desertification, with desertified land covering approximately 27.00% of its total area (Tu et al., 2016), primarily concentrated in arid and semi-arid areas like Inner Mongolia Autonomouse Region, Xinjiang Uygur Autonomouse Region, Xizang Autonomous Region, Qinghai Province, and Gansu Province (Shen, 2023). Among the broader desertification landscape in China, the desertification issues on the Qinghai-Xizang Plateau stand out due to its particularly distinct. The Qinghai-Xizang Plateau, known as the "Roof of the World", is a globally significant ecological barrier and biodiversity conservation area, and its environment plays a crucial role in global climate change (Lu et al., 2023). The climate of the Qinghai-Xizang Plateau is cold and arid, belonging to a fragile ecosystem.

Desertification affects approximately 3.93×10^5 km^2 of the Qinghai-Xizang Plateau, mainly concentrated in valleys, basins, and around lakes (Zhang et al., 2018; Lu et al., 2023; Shen, 2023). Previous studies of desertification on the Qinghai-Xizang Plateau primarily cover aeolian processes during geological history and modern land desertification. Stratigraphic profiles constitute the primary evidence for the study of aeolian activity and desertification since geological periods (Liu et al., 2013). Researchers have studied aeolian profiles in areas such as the Qaidam Basin (Chen et al., 2016), the Qinghai Lake basin (Lu et al., 2010), and the Yarlung Zangbo River valley (Ling et al., 2019), thereby revealing aeolian activity and environmental evolution since geological periods. Previous studies of modern desertification on the Qinghai-Xizang Plateau include the mechanisms of desertification formation (Li et al., 1999), desertification monitoring and assessment (Wang et al., 2015), influencing factors (Hu et al., 2011), and preventive measures (Dong, 2001). With the advancement of ecological civilization construction, the monitoring and assessment of desertification, as a prerequisite for implementing desertification control measures and a crucial process in evaluating the effectiveness of ecological restoration, has gradually become a focal points in ecological research on the Qinghai-Xizang Plateau (Wang, 2004; Wei et al., 2019). Using remote sensing and geographic information technologies, researchers can access remote sensing data at larger spatial and temporal scales, enabling dynamic desertification monitoring (Wang et al., 2015; Zhang et al., 2018). Furthermore, the application of multi-source data fusion technology enhances the comprehensiveness and accuracy of desertification monitoring and assessment (Ren et al., 2024). A review of existing research reveals that desertification monitoring and assessment on the Qinghai-Xizang Plateau has expanded from local areas, such as the Qinghai Lake basin (Wang et al., 2015), the source region of the Yellow River (Hu et al., 2011), and the Gonghe Basin (Li et al., 2018) to the entire plateau (Li et al., 2016; Zhang et al., 2018). However, the indicators used for desertification monitoring and assessment are not standardized, and there are inconsistencies in the types and severity levels of classification. The distinctive geographic and climatic conditions of the Qinghai-Xizang Plateau necessitate the development of more detailed standards for desertification monitoring and assessment to address regional variations and offer a scientific foundation for desertification control.

Desertification sensitivity, as an important indicator for quantifying the degree of desertification, is used to assess the likelihood of land becoming desertified and has become a focal point for many researchers (Sterk et al., 2016). Methods for studying desertification sensitivity include the environmental sensitivity area index (ESAI) (Kosmas et al., 1999), the desertification sensitivity index (DSI) derived from the spatial overlay analysis method (Liu et al., 2002), and sensitivity evaluation systems based on the "Pressure-State-Response" framework (Tian et al., 2018). ESAI is particularly popular due to its flexible indicator selection and efficient computation (Ding et al., 2020; Shao et al., 2023). However, ESAI was originally developed in the Mediterranean region, which was not used in the other areas (Prăvălie et al., 2017; Xu et al., 2019).

Improving the desertification sensitivity evaluation system by optimizing evaluation indicators and methods to enhance the objectivity and comprehensiveness of the results is necessary. This study focuses on the Qinghai-Xizang Plateau, selecting topography, climate, soil, hydrology, and vegetation as evaluation indicators, and constructs a desertification sensitivity evaluation system based on ESAI and spatial distance models to address the following issues: (1) the spatiotemporal variation characteristics of desertification sensitivity on the Qinghai-Xizang Plateau from 1990 to 2020; and (2) the effects of influencing factors and their interactions on the changes in desertification sensitivity, and the contribution of each factor. The results will provide theoretical support for desertification control efforts on the Qinghai-Xizang Plateau.

2 Materials and methods

2.1 Study area

The Qinghai-Xizang Plateau is located in southwestern China (26°00′–39°47′N, 73°19′–104°47′E) and spans six provinces and autonomous regions: Qinghai Province, Xizang Autonomous Region, Xinjiang Uygur Autonomous Region, Sichuan Province, Gansu Province, and Yunnan Province (Teng et al., 2021). The Qinghai-Xizang Plateau features a complex terrain, surrounded by an intricate interplay of mountains, basins, and valleys (Yao et al., 2012; Zhang et al., 2018). The climate of the Qinghai-Xizang Plateau is influenced by the East Asian monsoon, the Indian monsoon, and westerlies, with an annual mean temperature ranging from –5.6°C to 17.6°C (Zhang et al., 2018; Lu et al., 2023). Mean annual precipitation decreases gradually from southeast to northwest, with the southeastern area receiving over 2000 mm and northwestern area receiving 20–75 mm of precipitation (Huang et al., 2016). The soil exhibits distinct vertical zonation, with alpine soil being the most prevalent type. Grassland is the predominant land use type on the Qinghai-Xizang Plateau (Teng et al., 2021), covering 51.40% of the total area in 2020.

2.2 Data sources

In this study, the data included topography, soil, hydrology, climate, vegetation, and socioeconomy. Digital elevation model (DEM) was obtained from the Geospatial Data Cloud (http://www.gscloud.cn), while aspect and slope were obtained using the "slope" and "aspect" tools in ArcGIS v.10.8 software (Wei et al., 2021). Soil depth, sand content, and organic matter content were obtained from the National Tibetan Plateau Data Center (http://data.tpdc.ac.cn). Soil erosion intensity data were obtained from the Resource Environment Data Center of Chinese Academy of Sciences (http://www.resdc.cn). River data come from the National Geomatic Information Center of China (http://www.ngcc.cn), and the lakes, reservoirs, glaciers, and snow data were extracted by ArcGIS software (Chen et al., 2019). Land use data were obtained from the Resource Environment Data Center of Chinese Academy of Sciences. The annual average wind speed, precipitation, air temperature, and ground temperature data from 1990 to 2020 were obtained from the meteorological station supplied by the National Meteorological Information Center (http://data.cma.cn). Vegetation data were obtained from the Resource Environment Data Center of Chinese Academy of Sciences. The Landsat data from the United States Geological Survey (http://landsatlook.usgs.gov/) were downloaded to calculate the normalized difference vegetation index (NDVI). The socioeconomic data were obtained from the Resource Environment Data Center of Chinese Academy of Sciences (http://www.resdc.cn). All the data were preprocessed with a specified coordinate system and a specified spatial resolution (1 km), which were all carried out in ArcGIS software.

2.3 Methods

2.3.1 Construction of a sensitivity evaluation system for desertification

Desertification sensitivity is the result of an interplay of multiple factors (Salvati and Bajocco, 2011; Karamesouti et al., 2018). The selection of research methods and indicators should fully consider

the environmental characteristics and current conditions of the study area (Ren et al., 2024). We obtained ESAI evaluation results based on the linear weighted sum and geometric mean of the indicators, without considering the interrelationship between indicators (Xu et al., 2019; Shao et al., 2023). Integrating spatial distance model (SDM) in the evaluation systems can effectively resolve this issue (Mesquita et al., 2017). Spatial distance models have been widely used in the fields such as land desertification assessment and ecological sensitivity evaluation (Wei et al., 2019; Zhao et al., 2022; Jiang et al., 2023). The formula of the SDM is as follows:

$$\mathrm{SDM}=\sqrt[2]{\sum_{i=1}^{n}(\alpha_i-\alpha_{i\text{-low}})^2}\ , \tag{1}$$

where SDM is obtained by the Euclidean distance between point α_i and point $\alpha_{i\text{-low}}$ (km); $\alpha_{i\text{-low}}$ is the lowest reference point at point α_i; and n is the dimension of the space.

Based on this, the study integrates ESAI evaluation method with SDM to construct DSI using indicators of topography, soil, climate, hydrology, and vegetation. To confirm the suitability of DSI, we conducted a multivariate collinearity diagnosis of all indicators using SPSS v.26.0 software.

It was found that the variance inflation factors (VIF) of the selected indices were all less than 10.0, the tolerances were all greater than 0.1, and there was no obvious collinearity (Wang and Xu, 2017). Therefore, using DSI (dimensionless) to study desertification sensitivity in the Qinghai-Xizang Plateau is feasible. A higher DSI value indicates a greater degree of desertification sensitivity. The formula of DSI is as follows:

$$\mathrm{DSI}=\sqrt[2]{(\mathrm{VBI}-\mathrm{VBI}_{\mathrm{low}})^2+(\mathrm{CBI}-\mathrm{CBI}_{\mathrm{low}})^2+(\mathrm{HBI}-\mathrm{HBI}_{\mathrm{low}})^2+(\mathrm{SBI}-\mathrm{SBI}_{\mathrm{low}})^2+(\mathrm{TBI}-\mathrm{TBI}_{\mathrm{low}})^2}\ , \tag{2}$$

where VBI, CBI, HBI, SBI, and TBI are the vegetation, climatic, soil, hydrological, and topographic background indices, respectively (Table 1); and $\mathrm{VBI}_{\mathrm{low}}$, $\mathrm{CBI}_{\mathrm{low}}$, $\mathrm{HBI}_{\mathrm{low}}$, $\mathrm{SBI}_{\mathrm{low}}$, and $\mathrm{TBI}_{\mathrm{low}}$ are the lowest values of each background index.

Table 1 Construction methods for various indices

Background index	Formula	Index composition	Index processing	Index description
Vegetation background index (VBI)	$\mathrm{VBI}=\sqrt{\sum_{i=1}^{n}(V_i-V_{i\text{-low}})^2}$	Vegetation drought tolerance	+	Vegetation drought tolerance was determined by quantifying the types of vegetation (Li et al., 2018).
		NDVI	–	
Climatic background index (CBI)	$\mathrm{CBI}=\sqrt{\sum_{i=1}^{n}(C_i-C_{i\text{-low}})^2}$	Annual average ground temperature (°C)	+	Aridity index= $P/(t^0+10)$, where P is the mean annual precipitation (mm), and t^0 is the annual mean temperature (°C) (Zhang, 1994).
		Annual average wind speed (m/s)	+	
		Aridity index	–	
Hydrological background index (HBI)	$\mathrm{HBI}=\sqrt{\sum_{i=1}^{n}(H_i-H_{i\text{-low}})^2}$	Distance to glaciers (km)	+	The distances to glaciers, rivers, lakes, and reservoirs were calculated using the Euclidean distance tool in ArcGIS software (Wei et al., 2021).
		Distance to rivers (km)	+	
		Distance to lakes and reservoirs (km)	+	
Soil background index (SBI)	$\mathrm{SBI}=\sqrt{\sum_{i=1}^{n}(S_i-S_{i\text{-low}})^2}$	Soil organic matter content (%)	–	Soil organic matter content=soil organic carbon/0.58 (Wei et al., 2021).
		Soil erosion intensity	+	
		Soil sand content (%)	+	
		Soil depth (cm)	+	
Topographic background index (TBI)	$\mathrm{TBI}=\sqrt{\sum_{i=1}^{n}(T_i-T_{i\text{-low}})^2}$	Slope (°)	–	Aspect is assigned values as follows: flat=1; west, northwest, and north=2; northeast and east=3; southeast, south, and southwest=4 (Xu et al., 2019).
		Altitude (m)	–	
		Aspect	+	

Note: V_i, C_i, H_i, S_i, and T_i are the constitutive factors of VBI, CBI, HBI, SBI and TBI, respectively; $V_{i\text{-low}}$, $C_{i\text{-low}}$, $H_{i\text{-low}}$, $S_{i\text{-low}}$, and $T_{i\text{-low}}$ are the lowest values of V_i, C_i, H_i, S_i, and T_i, respectively; i is the constitutive factor; n is the total number of constitutive factors. "+" means the positive normalization, and "–" means the negative normalization. NDVI, normalized difference vegetation index.

In this study, the Jenks' natural break method was used to classify DSI into five classes (Shao et al., 2023; Ren et al., 2024): nonsensitivity (DSI≤1.272), mild sensitivity (1.272<DSI≤1.312), moderate sensitivity (1.312<DSI≤1.490), severe sensitivity (1.490<DSI≤1.708), and extreme sensitivity (1.708<DSI).

2.3.2 Gravity center transfer model

The model of gravity center transfer can be used to analyze the spatial evolution of elements (Saldarriaga and Hua, 2019; Fu et al., 2016). The formula is as follows:

$$X_{it}=\frac{\sum_{i=1}^{m}X_iP_i}{\sum_{i=1}^{m}P_i};\quad Y_{it}=\frac{\sum_{i=1}^{m}Y_iP_i}{\sum_{i=1}^{m}P_i}, \tag{3}$$

where X_{it} and Y_{it} are the Cartesian coordinates of the gravity center sensitive to type i desertification in year t; X_i and Y_i are the coordinates of the gravity center of small patches sensitive to type i desertification; P_i is the total area of desertification sensitivity type i (km^2); and m is the total number of desertification sensitivity type i patch.

2.3.3 Transfer matrix

Transfer matrix model was employed to quantitatively reveal the transfer of different desertification sensitivity types from the beginning to the end of the study (Jana et al., 2022). The formula is as follows:

$$A_{xy}=\begin{bmatrix} A_{11} & \cdots & A_{1a} \\ \vdots & \ddots & \vdots \\ A_{a1} & \cdots & A_{aa} \end{bmatrix}, \tag{4}$$

where A_{xy} is the probability of the transfer from type x to type y desert sensitivity in the study area (%); x is the desertification sensitivity type at the beginning; y is the desertification sensitivity type at the end; and a is the number of desertification sensitivity types.

2.3.4 Geodetector

Geodetector is a statistical method designed to detect spatial heterogeneity and identify its drivers (Wang et al., 2010). It has been extensively utilized in ecological and environmental research and offers significant advantages over traditional statistical methods in analyzing interactions among various factors (Wang and Xu, 2017; Chen et al., 2021). The formula for calculating the q-value is as follows:

$$q=1-\frac{\sum_{h=1}^{L}N_h\sigma_h^2}{N\sigma^2}, \tag{5}$$

where h=1, 2, …, L is the number of partitions of the influencing factors; N and N_h are the number of the whole region and subregions in class h, respectively; and σ^2 and σ_h^2 are the variances of the variables for the entire region and h layer, respectively. The q-values range between 0.0000 and 1.0000, with higher q-value indicates a stronger explanatory power of the factor.

3 Results

3.1 Topographic, soil, vegetation, climatic, and hydrological background indices

Spatial distribution of the five background indices in 2020 is shown in Figure 1. The Qinghai-Xizang Plateau features complex terrain, with TBI values ranging from 0.457 to 1.724. Topographic quality is poorer on sunny slopes compared with shady slopes and improves with increasing altitude and slope. SBI values ranged from 1.000 to 1.989, with the poorest soil quality

found primarily in the Qaidam Basin in the northeast. The Qinghai-Xizang Plateau has a wide variety of plant species and complex vegetation types. Forests were primarily concentrated in southern and southeastern areas, dominated by evergreen broadleaf and evergreen coniferous shrubs. The spatial distribution of CBI indicated better climatic quality near Three-River Headwaters region, decreasing in a banded pattern toward southeast and northwest. The distribution characteristics of HBI revealed that areas farther from major rivers, lakes, reservoirs, and glacier and snow cover areas exhibited superior hydrological quality. Figure 2 depicts the changes in the average values of each background index from 1990 to 2020. The results indicated that CBI on the Qinghai-Xizang Plateau showed significant fluctuations, with annual average values of 0.282, 0.424, 0.391, and 0.385 in 1990, 2000, 2010, and 2020, while the annual average values of SBI, TBI, VBI, and HBI showed smaller fluctuations. Annual average values of VBI on the Qinghai-Xizang Plateau were 0.758, 0.748, 0.755, and 0.735 in 1990, 2000, 2010, and 2020, respectively, indicating a decreasing trend with fluctuation, which reflected an overall improvement in vegetation quality over this period.

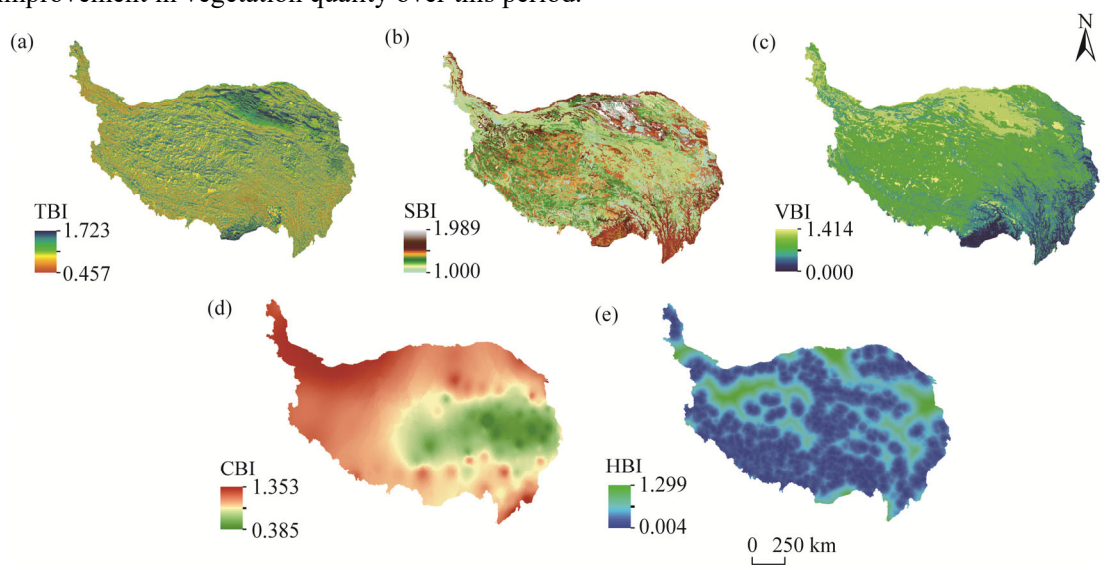

Fig. 1 Spatial distributions of the five background indices on the Qinghai-Xizang Plateau in 2020. (a), TBI (topographic background index); (b), SBI, (soil background index); (c), VBI (vegetation background index); (d), CBI (climatic background index); (e), HBI (hydrological background index). The abbreviations are the same in the following figures.

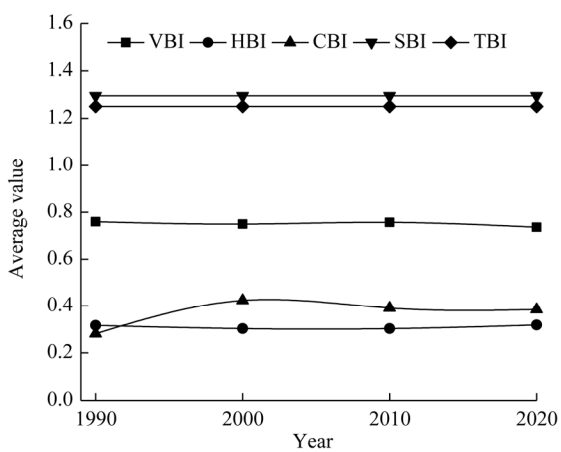

Fig. 2 Average values of the five background indices from 1990 to 2020. High values of the background index indicate poor quality.

3.2 Spatial distribution of desertification sensitivity

Figure 3 illustrates the spatial distribution of desertification sensitivity on the Qinghai-Xizang Plateau from 1990 to 2020. The overall distribution of desertification sensitivity showed higher sensitivity in the northwest and lower sensitivity in the southeast. In the southeastern forests, desertification sensitivity was lower, while it increased as desertification intensified toward the northwest. Specifically, low-sensitivity desertification areas (including areas of nonsensitivity and mildly sensitivity) were mainly located in the Hengduan Mountains, Nyainqêntanglha Mountains, and their surrounding meadows and forests with high vegetation cover in the southeast. High-sensitivity desertification areas (including areas of extreme and severe sensitivity) were mainly distributed in the Kunlun Mountains, Altun Mountains, and adjacent desertified areas in the northwest. Desertification sensitivity was most severe in the Qaidam Basin and northwestern area. Desertified land types in severely sensitive areas were mainly concentrated on the land with gravels, bare land, and fixed sandy land. In areas of extreme sensitivity, the dominant land types were the bare land with gravels, degraded land caused by wind erosion, and mobile sandy land.

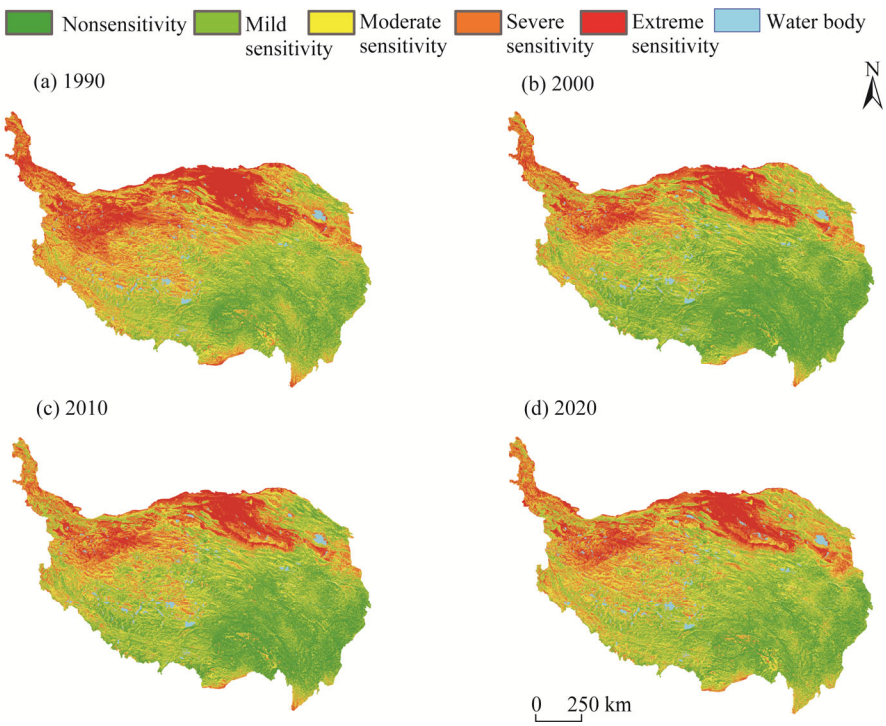

Fig. 3 Spatial distribution of desertification sensitivity index (DSI) on the Qinghai-Xizang Plateau from 1990 to 2020. (a), 1990; (b), 2000; (c), 2010; (d), 2020.

To further understand the spatial evolution of desertification sensitivity on the Qinghai-Xizang Plateau from 1990 to 2020, we utilized the gravity center transfer model to analyze the distribution of gravity centers for various types of desertification sensitivity over the past 30 a (Fig. 4). From 1990 to 2000, all types of desertification sensitivity migrated to the northwest, with the most significant degree of movement observed, indicating the most rapid improvement in desertification during this period. Overall, the centroids of all types of desertification-sensitive areas migrated to the northwest from 1990 to 2020, signifying an expansion of nonsensitive areas and a reduction in extremely sensitive areas, suggesting a decreasing trend in land desertification on the Qinghai-Xizang Plateau.

3.3 Temporal variation of desertification sensitivity

Table 2 illustrates the area proportions and dynamic degree results of different types of desertification

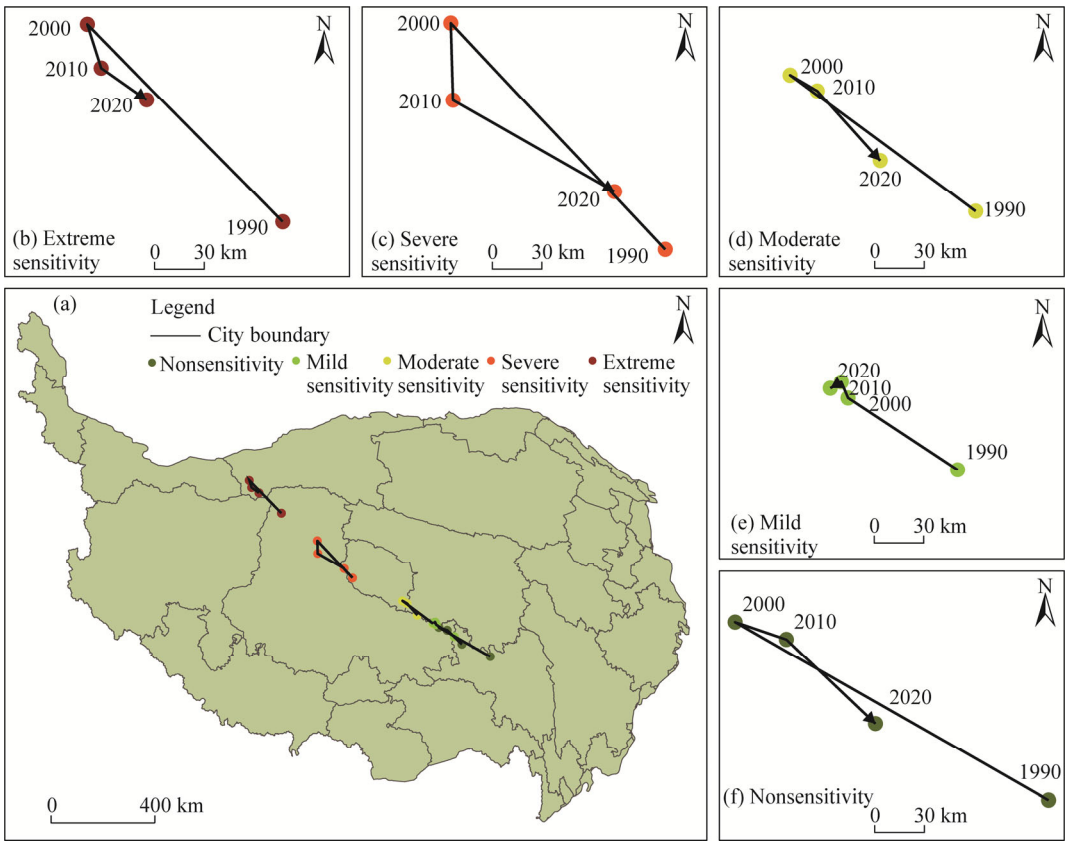

Fig. 4 Gravity center distribution of desertification sensitivity on the Qinghai-Xizang Plateau from 1990 to 2020. (a), overall distribution of desertification sensitivity; (b), extreme sensitivity; (c), severe sensitivity; (d), moderate sensitivity; (e), mild sensitivity; (f), nonsensitivity. The map is provided by the National Tibetan Plateau Data Center (http://data.tpdc.ac.cn/) and the boundary of the map is not modified.

Table 2 Area proportion and dynamic degree of desertification sensitivity on the Qinghai-Xizang Plateau from 1990 to 2020

Desertification sensitivity type	Area proportion (%)				Dynamic degree (%)
	1990	2000	2010	2020	1990–2020
Nonsensitivity	8.74	19.66	16.55	10.88	0.66
Mild sensitivity	22.91	29.88	30.42	28.24	0.63
Moderate sensitivity	30.35	25.50	27.36	31.26	0.10
Severe sensitivity	24.04	16.30	17.05	20.29	–0.62
Extreme sensitivity	13.95	8.67	8.62	9.33	–1.65

sensitivity on the Qinghai-Xizang Plateau from 1990 to 2020. From 1990 to 2000, the areas of nonsensitivity and mild sensitivity increased by 10.92% and 6.92%, respectively, indicating a reduction in desertification sensitivity. From 2010 to 2020, the areas of nonsensitivity and mild sensitivity decreased by 5.67% and 2.18%, respectively, suggesting an increase in desertification sensitivity during this period. Overall, the average values of the DSI from 1990 to 2020 indicated a decreasing trend, with values from 1.438 to 1.389. The areas of nonsensitivity, mild sensitivity, and moderate sensitivity increased by 2.14%, 5.33%, and 0.91%, respectively, with dynamic degrees of 0.66%, 0.63%, and 0.10%. The dynamic degrees of severe sensitivity and extreme sensitivity were –0.62% and –1.65%, respectively, indicating an overall decreasing trend in desertification sensitivity in the Qinghai-Xizang Plateau from 1990 to 2020, with the most

significant changes observed in extremely sensitive areas.

The area proportions and dynamic degrees of desertification sensitivity types only reveal changes within individual sensitivity types, making it difficult to identify transitions between them. Therefore, the transfer probability matrix of desertification sensitivity types was calculated using ArcGIS software (Table 3). From 1990 to 2020, the probabilities of transitioning from nonsensitivity to mild sensitivity, mild sensitivity to moderate sensitivity, moderate sensitivity to severe sensitivity, and severe sensitivity to extreme sensitivity were 7.89%, 3.54%, 1.51%, and 0.31%, respectively. In contrast, the probabilities of transitioning from extreme sensitivity to severe sensitivity, severe sensitivity to moderate sensitivity, moderate sensitivity to mild sensitivity, and mild sensitivity to nonsensitivity were 33.56%, 36.56%, 27.11%, and 12.28%, respectively. This result suggests that over the past 30 a, the desertification sensitivity on the Qinghai-Xizang Plateau has shown a greater shift to a lower sensitivity level. Overall, from 1990 to 2020, 24.56% of the Qinghai-Xizang Plateau experienced a reduction in desertification sensitivity, shifting from high risk to low risk, while only 2.03% of the area experienced an increase, moving from low risk to high risk.

Table 3 Transfer probability matrix of desertification sensitivity types on the Qinghai-Xizang Plateau from 1990 to 2020

Desertification sensitivity type	Nonsensitivity	Mild sensitivity	Moderate sensitivity	Severe sensitivity	Extreme sensitivity
			(%)		
Nonsensitivity	92.10	7.89	0.00	0.00	0.00
Mild sensitivity	12.28	84.18	3.54	0.00	0.00
Moderate sensitivity	0.05	27.11	71.32	1.51	0.00
Severe sensitivity	0.00	0.12	36.56	63.01	0.31
Extreme sensitivity	0.00	0.00	0.03	33.56	66.41

3.4 Change in desertification sensitivity

To further explore the changes of desertification sensitivity on the Qinghai-Xizang Plateau, this study used ArcGIS software to classified desertification sensitivity into stabilizing type I, decreasing type, fluctuating type, increasing type, and stabilizing type II (Table 4; Fig. 5).

From 2000 to 2020, desertification sensitivity demonstrated significant temporal and spatial variability, with the areas where desertification sensitivity types changed accounting for 53.00% of the total area. The order of changes was as follows: fluctuating type (28.70%)>decreasing type (23.30%)>increasing type (1.10%). The fluctuating type was widely distributed across the Qinghai-Xizang Plateau, characterized by an unstable desertification sensitivity that was highly susceptible to environmental changes. The decreasing type was primarily distributed around extreme sensitivity, showing that ecological engineering measures were effective to control dertification. The increasing type was mostly concentrated in densely populated areas, often close to roads. During the study period, 47.00% of the study area remained unchanged in terms of

Table 4 Classification of change types in desertification sensitivity

Change type	Meaning
Stabilizing type I	Sensitivity was perennially non-sensitive, mildly sensitive, and moderately sensitive
Decreasing type	Desertification sensitivity continued to decrease
Fluctuating type	Sensitivity fluctuated
Increasing type	Desertification sensitivity continued to increase
Stabilizing type II	Sensitivity was perennially severe and extreme

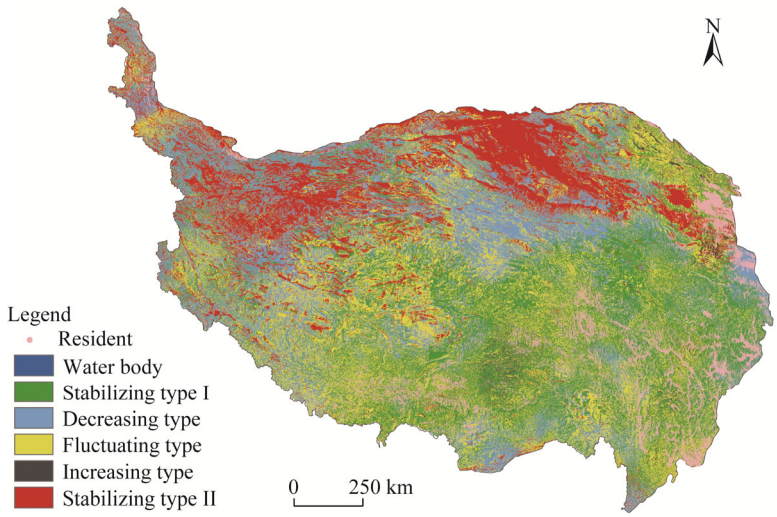

Fig. 5 Spatial distribution of change type in desertification sensitivity on the Qinghai-Xizang Plateau

desertification sensitivity. Stabilizing type I covered the largest area, primarily concentrated in the southeastern part of the study area, where the ecosystem was the most stable. Stabilizing type II was mainly distributed in the mountainous areas of northwestern and northern Qinghai-Xizang Plateau, particularly near the Qaidam Basin, where the climate was arid, vegetation was sparse, and desertification was severe. Overall, desertification sensitivity on the Qinghai-Xizang Plateau showed a decreasing trend, with some local areas experiencing an increased trend.

3.5 Factors influencing desertification sensitivity

This study selected 5 primary indicators and 17 secondary indicators, using the Geodetector to quantitatively analyze the internal and external factors influencing desertification sensitivity. The results of the factor detector (Table 5) indicated that the q-values rankings of different indicators vary across different periods. Among the primary indicators, VBI and CBI had higher q-values (0.4680 and 0.2600, respectively), underscoring the significant roles of vegetation and climate in the evolution of desertification sensitivity. Among the secondary indicators, aridity index had the highest q-value in 1990, while vegetation drought tolerance (VDT) had the highest q-value from 2000 to 2020. Their q-values were significantly higher than those of other factors, suggesting that aridity index and vegetation drought tolerance were the key factors influencing desertification sensitivity. From 1990 to 2020, the q-values of VDT ranged from 0.4672 to 0.5193, showing a trend of increasing fluctuation, while the q-values of aridity index ranged from 0.4755 to 0.3436, with a large fluctuation range, making it an active factor influencing desertification sensitivity. Other factors have a minor impact on desertification sensitivity (q-value<0.1800). Furthermore, gross domestic product (GDP) and population density did not pass the significance tests, implying that socioeconomic development had limited effects on desertification sensitivity.

The interaction results (Fig. 6) indicated that the q-value of VDT∩aridity index was greater than 0.6000, demonstrating that the combined effects of them significantly influenced desertification sensitivity. The interaction between each pair of secondary indicators on desertification sensitivity demonstrated either two-factor enhancement or nonlinear enhancement. Specifically, secondary indicators such as soil orgnic matter, soil depth, and altitude had relatively low impacts (q-value<0.1000). However, when these factors interacted with VDT or aridity index, their influence was amplified. The interaction detector also indicated that changes in desertification sensitivity resulted from the combined effects of multiple factors, rather than being driven by individual factor.

Table 5 *q*-values of interaction detector

Driving factor	1990	2000	2010	2020
VBI	0.4680	0.5025	0.5204	0.5036
NDVI	0.1923	0.2497	0.1945	0.1864
VDT	0.4672	0.5025	0.5193	0.5036
SBI	0.1325	0.1760	0.1760	0.1588
SOM	0.0887	0.0993	0.0962	0.0946
SE	0.0900	0.1073	0.1096	0.1034
SS	0.1282	0.1596	0.1593	0.1519
SD	0.0602	0.0710	0.0962	0.0726
TBI	0.1022	0.1033	0.1073	0.1163
AL	0.0736	0.0883	0.0822	0.0735
SL	0.1089	0.0984	0.1087	0.1083
AS	0.0411	0.0452	0.0464	0.0543
CBI	0.4704	0.4271	0.3843	0.2599
AI	0.4733	0.4755	0.4430	0.3436
WS	0.0719	0.0832	0.0900	0.0663
GT	0.0648	0.0817	0.0616	0.0676
HBI	0.1361	0.1644	0.1620	0.1633
DS	0.0097	0.0175	0.0199	0.0257
DR	0.1752	0.1714	0.1787	0.1664
DL	0.0202	0.0171	0.0137	0.0340
GDP	-	0.0002	0.0000	0.0002
POP	-	0.0005	0.0000	0.0005

Note: VDT, vegetation drought tolerance; SOM, soil organic matter; SE, soil erosion intensity; SS, soil sand; SD, soil depth; AL, altitude; SL, slope; AS, aspect; AI, aridity index; WS, wind speed; GT, annual average ground temperature; DS, distance to glaciers; DR, distance to rivers; DL, distance to lakes and reservoirs; GDP, gross domestic product; POP, population density. "-" means no value. The abbreviations are the same in the following figure.

4 Discussion

4.1 Variation of desertification sensitivity

Desertification sensitivity on the Qinghai-Xizang Plateau exhibited a general fluctuating downward trend from 1990 to 2020, with a significant decrease from 1990 to 2000 (average value of DSI decreased by 0.102) and a slight increase from 2010 to 2020 (average value of DSI increased by 0.039). This trend aligns with the findings of Teng et al. (2021). Teng et al. (2021) showed a general decreasing trend in wind erosion on the Qinghai-Xizang Plateau, with a significant reduction from 1990 to 2000, followed by an increase after 2010. The decrease in desertification sensitivity may be closely related to the implementation of various ecological projects (Wang et al., 2014; Guo et al., 2020; Yang et al., 2023), such as the Three-River Headwaters Ecological Protection and Restoration Project (1956–2000) and the Three-North Shelterbelt Program (1978–2050).

From 2010 to 2020, desertification sensitivity on the Qinghai-Xizang Plateau demonstrated an increasing trend. However, previous studies have reported an increase in vegetation coverage during this period (Ganjurjav et al., 2016; Guo et al., 2023), reflecting the complexity of variation in desertification sensitivity. The results from the factor detector revealed that from 2010 to 2020, the *q*-values for aspect, annual mean temperature, distance to glaciers, distance to lakes and reservoirs, gross domestic product, and population density increased. This result suggests that the

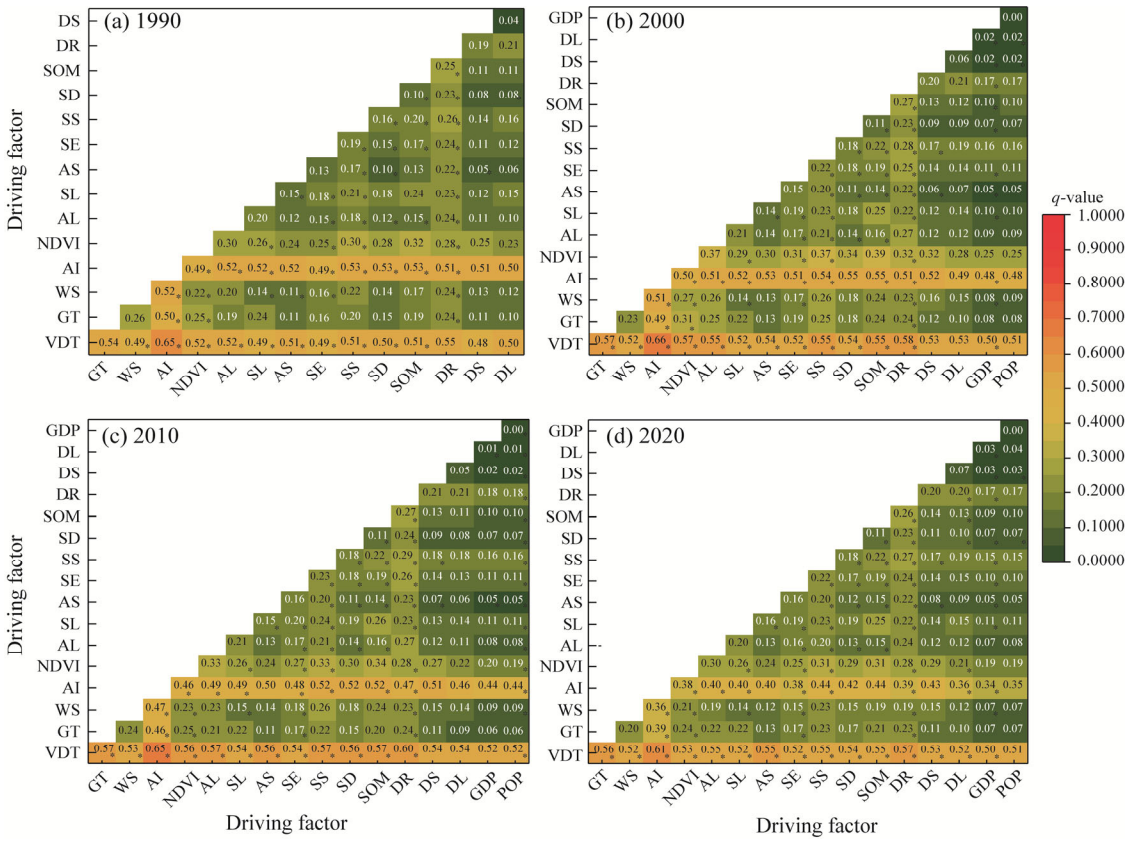

Fig. 6 Results of the interaction detector on the Qinghai-Xizang Plateau from 1990 to 2020. (a), 1990; (b), 2000; (c), 2010; (d), 2020. * is two-factor enhanced and the rest are nonlinear enhanced.

increase in desertification sensitivity may be closely related to rising temperature and intensified human activities. Rising temperature threatens permafrost stability, with highly unstable permafrost on the Qinghai-Xizang Plateau increasing by 6.09% from 2000 to 2019, leading to geological issues such as soil erosion, landslides, and water and soil loss (Wu et al., 2022; Yang et al., 2023), and increasing the potential for land desertification. In the context of climate change, the negative impacts of human activities on the natural environment are intensifying. Large-scale infrastructure construction, overgrazing, and deforestation have disrupted the ecological balance (Li et al., 2017; Shen et al., 2023), resulting in an increase in desertification sensitivity in localized areas.

4.2 Factors influencing the variation of desertification sensitivity

The variation in desertification sensitivity is influenced by multiple factors, with vegetation and climate identified as the primary influencing factors (Shao et al., 2023; Ren et al., 2024). In contrast to previous studies, this study selected more comprehensive and specific influencing factors and used geodetector for quantitative analysis, providing more accurate directions and a theoretical basis for desertification prevention and control on the Qinghai-Xizang Plateau.

The factor detector results indicate that vegetation drought tolerance and aridity index exhibited strong explanatory power for changes in desertification sensitivity on the Qinghai-Xizang Plateau. Vegetation drought tolerance directly affects plant growth, degradation, and recovery. Through mechanisms such as root system stabilizing soil and reducing wind erosion (Tang et al., 2019; Smit et al., 2024), plants effectively mitigate desertification that is exacerbated by climate change. The role of vegetation restoration in preventing land desertification is widely recognized in arid

and semi-arid areas (Wang et al., 2014; Wei et al., 2021). The aridity index reflects the combined effects of temperature and precipitation, the increasing trend in both temperature and precipitation on the Qinghai-Xizang Plateau has promoted vegetation coverage (Lu et al., 2023; Ren et al., 2024), indirectly influencing desertification sensitivity. Previous studies have shown that climate warming and wetting can effectively mitigate desertification processes on the Qinghai-Xizang Plateau (Li et al., 2016; Jiang et al., 2019). In contrast, gross domestic product and population density have exerted a relatively minor impact on desertification sensitivity. Human activities and economic development frequently disrupt the ecological environment in populated areas (Li et al., 2017; Wei et al., 2021), resulting in increased desertification sensitivity around settlements and roads. Interaction detector results indicate that the interactions between influencing factors exhibit either two-factor enhancement or nonlinear enhancement. The combined effect of vegetation drought tolerance and aridity index had the most significant impact on desertification sensitivity. This result highlights the importance of integrated management measures.

Overall, the variation in desertification sensitivity on the Qinghai-Xizang Plateau results from the combined effects of multiple factors. However, this study primarily focuses on natural factors and gives comparatively less attention to socioeconomic factors. In future studies, we will incorporate a more comprehensive set of socioeconomic factors, such as grazing and infrastructure development, to quantify their impact on changes in desertification sensitivity in densely populated areas and enhance our understanding of the driving mechanisms behind desertification.

5 Conclusions

This study constructed a desertification sensitivity evaluation system based on ESAI and spatial distance model to assess desertification sensitivity on the Qinghai-Xizang Plateau from 1990 to 2020. Additionally, the geodetector was used to quantitatively analyze the factors influencing desertification sensitivity. The spatial distribution of desertification sensitivity on the Qinghai-Xizang Plateau displayed a pattern of higher in the northwest and lower in the southeast, with the centers of different sensitivity areas moving toward the northwest. DSI on the Qinghai-Xizang Plateau fluctuated downward from 1990 to 2020, with a higher probability of desertification sensitivity shifting from high to low risk. However, in some localized areas, such as near settlements and roads, sensitivity has increased, highlighting the need for enhanced ecological protection and restoration. Vegetation and climate are the primary factors driving changes in desertification sensitivity on the Qinghai-Xizang Plateau, with vegetation drought tolerance and aridity index showing strong explanatory power. Furthermore, interactions among factors exhibit either two-factor or nonlinear enhancement, with the interaction between vegetation drought tolerance and aridity index having the most significant impact on sensitivity. This study revealed the variation in desertification sensitivity on the Qinghai-Xizang Plateau over the past 30 a, underscoring the dominant role of natural factors in the desertification process. The result provides not only scientific support for ecological management in the study area but also a crucial reference for ecosystem protection in arid areas globally. Future research should incorporate high-resolution remote sensing or field observation data to better examine the trends of desertification sensitivity and their key factors in different areas. Moreover, predictive analyses of desertification sensitivity under various climate scenarios should be enhanced to offer more targeted and forward-looking recommendations for ecological protection and restoration.

Conflict of interest

The authors declare that they have no known competing financial interests or personal relationships that could have appeared to influence the work reported in this paper.

Acknowledgements

This study was funded by the National Natural Science Foundation of China (42371219), the Key Natural Science Foundation of Gansu Province (24JRRA135), and the Oasis Scientific Research Achievements Breakthrough Action Plan Project of Northwest Normal University (NWNU-LZKX-202302).

Author contributions

Conceptualization: PAN Meihui; Methodology: PAN Meihui, CHEN Qing; Data curation: LI Chenlu, LI Na; Software: CHEN Qing, LI Chenlu; Formal analysis: PAN Meihui, CHEN Qing; Writing - original draft preparation: PAN Meihui, CHEN Qing; Writing - review and editing: PAN Meihui, CHEN Qing, LI Chenlu, LI Na, GONG Yifu; Funding acquisition: PAN Meihui. All authors approved the manuscript.

References

Chen F H, Wu S H, Cui P, et al. 2021. Progress and prospects of applied research on physical geography and the living environment in China over the past 70 years (1949–2019). Journal of Geographical Sciences, 31: 3–45.

Chen T, Song Y G, Li Y. 2016. Wind-blown sand activities in the Qaidam Basin during the Last Glacial Maximum and the Holocene Megathermal Period. Arid Zone Research, 33(4): 877–883. (in Chinese)

Chen W X, Li J F, Zeng J, et al. 2019. Spatial heterogeneity and formation mechanism of eco-environmental effect of land use change in China. Geographical Research, 38(9): 2173–2187. (in Chinese)

Ding J C, Chen Y Z, Wang X Q, et al. 2020. Land degradation sensitivity assessment and convergence analysis in Korla of Xinjiang, China. Journal of Arid Land, 12(4): 594–608.

Dong Y X. 2001. Study on the control of land desertification and its project construction in Tibet Autonomous Region. Journal of Natural Resources, 16(2): 145–151. (in Chinese)

Fu X, Shen Y, Dong R C, et al. 2016. Analysis of urbanization based on center-of-gravity movement and characteristics in Songhua River basin of China and its southern source sub-basin between 1990 and 2010. Chinese Geographical Science, 26(1): 117–128.

Ganjurjav H, Gao Q Z, Gornish E S, et al. 2016. Differential response of alpine steppe and alpine meadow to climate warming in the central Qinghai-Tibetan Plateau. Agricultural and Forest Meteorology, 223: 233–240.

Guo B, Zang W Q, Yang F, et al. 2020. Spatial and temporal change patterns of net primary productivity and its response to climate change in the Qinghai-Tibet Plateau of China from 2000 to 2015. Journal of Arid Land, 12(1): 1–17.

Guo J S, Sang H Y, Zhai L. 2023. Spatiotemporal variations and driving factors of vegetation coverage on the Qinghai-Tibet Plateau. Chinese Journal of Ecology, 42(11): 2665–2674. (in Chinese)

Hu G Y, Dong Z B, Lu J F, et al. 2011. Spatial and temporal changes of desertification land and its influence factors in source region of the Yellow River from 1975 to 2005. Journal of Desert Research, 31(5): 1079–1086. (in Chinese)

Huang K, Zhang Y J, Zhu J T, et al. 2016. The influences of climate change and human activities on vegetation dynamics in the Qinghai-Tibet Plateau. Remote Sensing, 8(10): 876, doi: 10.3390/rs8100876.

Jana A, Jat M K, Saxena A, et al. 2022. Prediction of land use land cover changes of a river basin using the CA-Markov model. Geocarto International, 37(26): 14127–14147.

Jiang L, Jiapaer G, Bao A M, et al. 2019. Monitoring the long-term desertification process and assessing the relative roles of its drivers in Central Asia. Ecological Indicators, 104: 195–208.

Jiang X H, Han L, Bai Z F, et al. 2023. Analysis of the temporal and spatial evolution pattern and trend of desertification sensitivity in the Inner Mongolia Autonomous Region. Acta Ecologica Sinica, 43(1): 364–378. (in Chinese)

Karamesouti M, Panagos P, Kosmas C. 2018. Model-based spatio-temporal analysis of land desertification risk in Greece. Catena, 167: 266–275.

Kosmas C, Kirkby M, Geeson N. 1999. The MEDALUS Project: Mediterranean Desertification and Land Use. Manual on Key Indicators of Desertification Mapping Environmental Sensitive Areas to Desertification. Luxembourg: Office for Official Publications of the European Communities.

Li D J, Xu D Y, Ding X, et al. 2018. Changes of wind erosion climatic erosivity and vegetation dynamics response in northern China from 1981 to 2010. Research of Soil and Water Conservation, 25(2): 15–20. (in Chinese)

Li Q, Zhang C L, Shen Y P, et al. 2016. Quantitative assessment of the relative roles of climate change and human activities in desertification processes on the Qinghai-Tibet Plateau based on net primary productivity. Catena, 147: 789–796.

Li S, Dong G R, Shen J Y, et al. 1999. The formation mechanism and development pattern of aeolian landforms in the Yarlung Zangbo River Valley. Science in China (Series D), 29(1): 88–96. (in Chinese)

Li Y, Zhou J, Wu X. 2017. Effects of the construction of Qinghai-Tibet railway on the vegetation ecosystem and eco-resilience. Geographical Research, 36(11): 2129–2140.

Ling Z Y, Jin J H, Wu D, et al. 2019. Aeolian sediments and their paleoenvironmental implication in the Yarlung Zangbo catchment (southern Tibet, China) since MIS3. Acta Geographica Sinica, 74(11): 2385–2400. (in Chinese)

Liu K, Xu W H, Ouyang Z Y, et al. 2002. GIS-based assessment on sensitivity to land desertification in Gansu Province. Bulletin of Soil and Water Conservation, 22(5): 29–31, 35. (in Chinese)

Liu X, Song L, Jin Y, et al. 2013. History of aeolian deposits in Tibetan Plateau and climate change over Holocene. Journal of Arid Land Resource and Environment, 27: 41–47. (in Chinese)

Lu H Y, Zhao C F, Mason J, et al. 2010. Holocene climatic changes revealed by aeolian deposits from the Qinghai Lake area (northeastern Qinghai-Tibetan Plateau) and possible forcing mechanisms. The Holocene, 21(2): 297–304.

Lu R R, Dai E F, Wu C S. 2023. Spatial and temporal evolution characteristics and driving factors of soil conservation services on the Qinghai-Tibet Plateau. Catena, 221: 106766, doi: 10.1016/j.catena.2022.106766.

Mesquita D P P, Gomes J P P, Junior A H S, et al. 2017. Euclidean distance estimation in incomplete datasets. Neurocomputing, 248: 11–18.

Prăvălie R, Săvulescu I, Patriche C, et al. 2017. Spatial assessment of land degradation sensitive areas in southwestern Romania using modified MEDALUS method. Catena, 153: 114–130.

Ren Y, Zhang B, Chen X D, et al. 2024. Analysis of spatial-temporal patterns and driving mechanisms of land desertification in China. Science of the Total Environment, 909: 168429, doi: 10.1016/j.scitotenv.2023.168429.

Saldarriaga J F, Hua Y. 2019. A gravity model analysis of forced displacement in Colombia. Cities, 95: 102407, doi: 10.1016/j.cities.2019.102407.

Salvati L, Bajocco S. 2011. Land sensitivity to desertification across Italy: Past, present, and future. Applied Geography, 31(1): 223–231.

Shao W Y, Wang Q Z, Guan Q Y, et al. 2023. Environmental sensitivity assessment of land desertification in the Hexi Corridor, China. Catena, 220: 106728, doi: 10.1016/j.catena.2022.106728.

Shen Y L. 2023. Study on influencing factors of spatial distribution of aeolian desertification in Qinghai-Tibetan Plateau. MSc Thesis. Zhejiang: Zhejiang Normal University. (in Chinese)

Smit M, Malan P, Smit N, et al. 2024. Response of herbaceous vegetation in the southern Kalahari following a prolonged drought. Journal of Arid Environments, 222: 105157, doi: 10.1016/j.jaridenv.2024.105157.

Sterk G, Boardman J, Verdoodt A. 2016. Desertification: History, causes and options for its control. Land Degradation & Development, 27(8): 1783–1787.

Tang Q H, Lan C, Su F G, et al. 2019. Streamflow change on the Qinghai-Tibet Plateau and its impacts. Chinese Science Bulletin, 64(27): 2807–2821. (in Chinese)

Teng Y M, Zhan J Y, Liu W, et al. 2021. Spatiotemporal dynamics and drivers of wind erosion on the Qinghai-Tibet Plateau, China. Ecological Indicators, 123: 107340, doi: 10.1016/j.ecolind.2021.107340.

Tian L, Qiu S J, Peng J, et al. 2018. Desertification sensitivity evaluation in Inner Mongolia Autonomous Region based on PSR framework. Progress in Geography, 37(12): 1682–1692. (in Chinese)

Tu Z F, Li M X, Sun T. 2016. The status and trend analysis of desertification and sandification. Forest Resources Management, 45(1): 1–5. (in Chinese)

UNCCD (United Nations Convention to Combat Desertification). 1994. Intergovernmental Negotiating Committee for a Convention to Combat Desertification, Elaboration of an International Convention to Combat Desertification in Countries Experiencing Serious Drought and/or Desertification, Particularly in Africa. New York: United Nations.

Wang H B, Ma M G, Geng L Y. 2015. Monitoring the recent trend of aeolian desertification using Landsat TM and Landsat 8 imagery on the north-east Qinghai-Tibet Plateau in the Qinghai Lake basin. Natural Hazards, 79: 1753–1772.

Wang J F, Li X H, Christakos G, et al. 2010. Geographical detectors-based health risk assessment and its application in the neural tube defects study of the Heshun Region, China. International Journal of Geographical Information Science, 24(1): 107–127.

Wang J F, Xu C D. 2017. Geodetector: Principle and prospective. Acta Geographica Sinica, 72(1): 116–134. (in Chinese)

Wang T. 2004. Progress in sandy desertification research of China. Journal of Geographical Sciences, 14: 387–400.

Wang Y H, Zhang L B, Guo Y, et al. 2014. Analysis of spatiotemporal pattern and tendency of land desertification sensitivity in

six provinces of China. Research of Soil and Water Conservation, 21(5): 132–137. (in Chinese)

Wei W, Guo Z C, Xie B B, et al. 2019. Spatiotemporal evolution of environment based on integrated remote sensing indexes in arid inland river basin in Northwest China. Environmental Science and Pollution Research, 26: 13062–13084.

Wei W, Guo Z C, Shi P J, et al. 2021. Spatiotemporal changes of land desertification sensitivity in northwest China from 2000 to 2017. Journal of Geographical Sciences, 31: 46–68.

Wu T H, Ma W S, Wu X D, et al. 2022. Weakening of carbon sink on the Qinghai-Tibet Plateau. Geoderma, 412: 115707, doi: 10.1016/j.geoderma.2022.115707.

Xu D Y, You X G, Xia C L. 2019. Assessing the spatial-temporal pattern and evolution of areas sensitive to land desertification in North China. Ecological Indicators, 97: 150–158.

Yang L, Zhao G, Mu X, et al. 2023. Integrated assessments of land degradation on the Qinghai-Tibet plateau. Ecological Indicators, 147: 109945, doi:10.1016/j.ecolind.2023.109945.

Yao T D, Thompson L G, Mosbrugger V, et al. 2012. Third pole environment (TPE). Environmental Development, 3: 52–64.

Zhang C L, Li Q, Shen Y P, et al. 2018. Monitoring of aeolian desertification on the Qinghai-Tibet Plateau from the 1970s to 2015 using Landsat images. Science of the Total Environment, 619–620: 1648–1659.

Zhang X S. 1994. Principles and optimal models for development of Maowusu sandy grassland. Chinese Journal of Plant Ecology, 18(1): 1–16. (in Chinese)

Zhao Z Y, Zhang Y T, Li T, et al. 2022. Comprehensive evaluation and spatio-temporal variations of ecological sensitivity on the Qinghai-Tibet Plateau based on spatial distance index. Acta Ecologica Sinica, 42(18): 7403–7416. (in Chinese)